Broad P V Absorption in the BALQSO, PG 1254+047: Column Densities, Ionizations and Metal Abundances in BAL Winds

Fred Hamann

Center for Astrophysics and Space Sciences University of California, San Diego; La Jolla, CA 92093-0424 Internet: fhamann@ucsd.edu

ABSTRACT

This paper discusses the detection of P V $\lambda\lambda 1118,1128$ and other broad absorption lines (BALs) in archival HST spectra of the low-redshift BALQSO, PG 1254+047. The P V identification is secured by excellent redshift and profile coincidences with the other BALs, such as C IV $\lambda\lambda 1548,1550$ and Si IV $\lambda\lambda 1393,1403$, and by photoionization calculations showing that other lines near this wavelength, e.g. Fe III $\lambda 1123$, should be much weaker than P V. The observed BAL strengths imply that either 1) there are extreme abundance ratios such as $[C/H] \gtrsim +1.0$, $[Si/H] \gtrsim +1.8$ and $[P/C] \gtrsim +2.2$, or 2) at least some of the lines are much more optically thick than they appear.

I argue that the significant presence of P V absorption indicates severe line saturation, which is disguised in the observed (moderate-strength) BALs because the absorber does not fully cover the continuum source(s) along our line(s) of sight. The variety of observed BAL strengths and profiles results from a complex mixture of ionization, optical depth and coverage fraction effects, making useful determinations of the abundance ratios impossible without a specific physical model. Computed optical depths for all UV resonance lines show that the observed BALs are consistent with solar abundances if 1) the ionization parameter is at least moderately high, $\log U \gtrsim -0.6$, 2) the total hydrogen column density is $\log N_{\rm H}({\rm cm}^{-2}) \gtrsim$ 22.0, and 3) the optical depths in strong lines like C IV and O VI $\lambda\lambda 1032,1038$ are $\gtrsim 25$ and ≥ 80 , respectively. These optical depths and column densities are at least an order of magnitude larger than expected from the residual intensities in the BAL troughs, but they are consistent with the large absorbing columns derived from X-ray observations of BALQSOs. In particular, a nominal X-ray column density of $\log N_{\rm H}({\rm cm}^{-2}) \sim 23$ could produce the observed BAL spectrum if $+0.4 \lesssim \log U \lesssim +0.7$ in a simple one-zone medium. The outflowing BALR, at velocities from -15,000 to -27,000 km s⁻¹ in PG 1254+047, is therefore a strong candidate for the X-ray absorber in BALQSOs.

Subject headings: Quasars: absorption lines; Quasars: general; Quasars: individual (PG 1254+047)

1. Introduction

Broad absorption lines (BALs) are prominent features in the UV spectra of ~10 to 15% of optically-selected (radio-quiet) QSOs (Foltz et al. 1990, Weymann et al. 1991). The lines form in ionized winds where the speeds can range from near zero to more than 30,000 km s⁻¹ (see Weymann 1995, Turnshek 1995, Turnshek 1988, Weymann, Turnshek & Christiansen 1985 for reviews). The most frequently measured lines are resonance transitions of H I (Ly α λ 1216) and moderate- to high-ionization metals such as C IV $\lambda\lambda$ 1548,1550, Si IV $\lambda\lambda$ 1393,1404,

N V $\lambda\lambda 1239,1243$ and O VI $\lambda\lambda 1032,1038$. Lower ionization lines such as Mg II $\lambda\lambda 2796,2804$ and Al III $\lambda\lambda 1855,1863$ are also detected in $\sim 15\%$ of BALQSOs in the optically-selected samples.

One of the most surprising results from BAL studies is the extreme elemental abundances implied by the absorption-line column densities (Weymann et al. 1985, Junkkarinen, Burbidge & Smith 1987, Turnshek 1988). Recent photoionization calculations that explore a wide range of ionization states and ionizing QSO spectral shapes (Korista et al. 1996, Turnshek et al. 1996, Hamann 1997) show, for example, that the measured ratios of Si IV to H I column densities require typical minimum Si/H abundances of $1.3 \leq [Si/H] \leq 2.0$, where [Si/H]is the logarithmic abundance ratio relative to solar, $\log (Si/H) - \log (Si/H)_{\odot}$. The surprising detections of broad P V $\lambda\lambda$ 1118,1128 absorption in PG 0946+301 (Junkkarinen et al. 1995, Junkkarinen et al. 1997) and possibly Q 1413+113 (Turnshek 1988) and Q 0226-104 (Korista et al. 1992) indicate an even more extreme situation where phosphorus is highly overabundant, with $[P/C] \gtrsim 1.8$ and $[P/H] \gtrsim 3.0$ independent of the uncertain ionization state (see also Hamann 1997 and §6 below).

Abundance determinations are important because they provide clues to the origin of the BAL gas, the physics of the acceleration mechanism and, perhaps, the nature of star formation and galactic nuclear evolution at high redshifts. Hamann & Ferland (1993) and Hamann (1997) showed that gas-phase metallicities up to $\sim \! \! 10 \ Z_{\odot}$ in QSOs are consistent with the vigorous star formation expected in the cores

of young massive galaxies. However, the extreme abundances derived for the BAL regions (BALRs) require a more exotic enrichment scenario. Gas-phase metallicities above 10 Z_{\odot} could, in principle, be reached by stellar populations with initial mass functions that are heavily weighted toward massive stars; but the overabundance of phosphorus is not compatible with any enrichment scheme dominated by Types I or II supernovae or by CNO-processed material from stellar envelopes. One possible solution, suggested by Shields (1996), is that the BAL gas is enriched by dwarf novae. Shields (1996) proposed that the needed high nova rates (relative to supernova rates) might be achieved near QSOs by white dwarfs gaining mass as they plunge through the accretion disk that surrounds the black hole. The overall feasibility of the nova hypothesis has not been tested, but it is clear that the high metallicities and P/C ratios estimated for the BALR are at least consistent with nova abundances.

Another possibility is that the BAL abundance results are simply incorrect. The abundance analysis hinges critically on the column densities derived from the residual intensities in BAL troughs. Typical estimates are $15.5 \leq \log N(\mathrm{cm}^{-2}) \leq 16.5$ for C IV, N V, and O VI, with smaller values by roughly 0.5 dex for H I and by ~ 1.0 dex for Si IV (Turnshek 1984, Weymann et al. 1985, Junkkarinen et al. 1987, Turnshek 1988, Korista et al. 1992, Hamann 1997). Estimates of the total hydrogen column densities (H I+H II) depend further on the uncertain ionization and/or metal abundances, but typical values are in the range $19 \leq \log N_{\rm H}(\mathrm{cm}^{-2}) \leq 20$.

It has long been recognized that these column densities are only lower limits (for example Junkkarinen et al. 1983 and 1987). High resolution spectroscopy has essentially ruled out the possibility that BAL troughs are composed of many unresolved components that "hide" large column densities (Barlow & Junkkarinen 1994). However, resolved narrow and intermediate-width line components in a few BALQSOs (Wampler et al. 1995, Barlow & Junkkarinen 1994) reveal multiplet ratios that require large optical depths, even though the lines appear too shallow to be optically thick (also Korista et al. 1992). Similar evidence has been noted in non-

BAL (exclusively narrow) absorption-line systems that are also known or suspected of forming in QSO outflows (Wampler et al. 1993, Petitjean et al. 1994, Barlow & Sargent 1997, Barlow, Hamann & Sargent 1997a, Hamann et al. 1997a, Hamann, Barlow & Junkkarinen 1997b, and Hamann et al. 1997c). These results imply that the line-absorbing regions do not fully cover the background emission source(s); some of the flux emerges unabsorbed and fills in the bottoms of the absorption troughs. Large line optical depths and partial line-of-sight coverage of the emitting source(s) are also suggested by curiously similar line depths in different BAL troughs and by BAL profiles that have nearly flat bottoms but fail to reach zero intensity (see Arav 1997).

Similar conclusions have been drawn from spectropolarimetry, where higher percentage polarizations are often measured in BAL troughs compared to the adjacent continuum. Evidently, some of the continuum flux is not absorbed by the BAL gas – perhaps because it is reflected into our line-of-sight by an extended scattering region (Cohen et al. 1995, Goodrich & Miller 1995, Hines & Wills 1995). The BALR might absorb the direct continuum radiation while the indirect (reflected) light is unabsorbed and thereby dilutes the observed BALs. The polarization and spectroscopic data therefore both indicate that the line optical depths and ionic column densities are larger than expected from the measured depths of the BALs.

Consistent with these findings, theoretical analysis of low-ionization BAL systems (with Mg II etc.) predicts that those BALRs should be optically thick at the Lyman edge (for roughly solar metallicities; Voit et al. 1993). For a nominal BAL profile width of 10,000 km s⁻¹, Ly α will be ~20 times more optically thick than the Lyman limit. Therefore, Ly α should be very saturated (in at least these low-ionization systems) even though it typically has a modest absorption depth in observed spectra (Weymann et al. 1991). This discrepancy between the observed and predicted Ly α troughs is probably due to partial line-of-sight coverage.

Additional evidence for large absorbing columns has come from observations showing that BALQ-SOs are significantly weaker soft X-ray sources

than non-BALQSOs with similar redshifts, luminosities and radio properties (Kopko et al. 1994, Green & Mathur 1996, Green et al. 1997). The spectral similarity of BAL and non-BAL QSOs in other bandpasses (e.g. Weymann et al. 1991) suggests that the difference in soft X-rays is caused by absorption rather than weaker emission in the BALQSOs. The implied X-ray absorbing columns are $\log N_{\rm H}({\rm cm}^{-2}) \gtrsim 22.3$ (for solar abundances; Green & Mathur 1996). In the two BALQSOs where soft X-rays are actually detected (Singh et al. 1987, Mathur et al. 1995, Green & Mathur 1996), absorption is clearly indicated with a total column density of $\log N_{\rm H}({\rm cm}^{-2}) \sim 23.1$ in both cases. The ionization state of the X-ray absorber is unknown, but Mathur et al. (1995) and Green & Mathur (1996) have suggested that it is similar to the highly-ionized ("warm") absorbers measured in soft X-ray spectra of many Seyfert 1 galaxies and a few low-redshift non-BALQSOs. (see Mathur 1994, Mathur et al. 1994, Laor et al. 1997, George et al. 1997, Reynolds 1997 and references therein). If the high column density X-ray absorption in BALQSOs occurs within the BALR, the amount of high-velocity outflowing material would be orders of magnitude larger than previous estimates based on the BALs alone.

This paper discusses the detection and implications of broad P V absorption in a low-redshift BALQSO, PG 1254+047 (V=15.8, $z_{em}=1.010$; Hewitt & Burbidge 1993). I argue that the detection of P V absorption, and in particular its strength relative to Si IV and C IV, is not a signal of unusual abundances but rather of line optical depths and column densities that are at least ten times larger than the standard estimates.

Sections 2-4 present the data and discuss the BAL profiles and identifications. Section 5 provides the standard analysis, with optical depths and column densities derived from the BAL troughs and photoionization calculations that constrain the ionization and metal abundances. This analysis leads to the relatively low column densities and extreme abundances described above. Section 6 reexamines the BAL data assuming the abundance ratios are roughly solar. That assumption leads to higher esti-

mates of the ionization, column densities and line optical depths. Section 7 discusses some implications of these results and §8 provides a summary.

2. The HST Archival Spectrum

PG 1254+047 was observed with the *Hubble* Space Telescope (HST) as part of the Absorption Line Key Project (Bahcall et al. 1993) on 17 February 1993. Spectra were obtained with the Faint Object Spectrograph (FOS) using the high-resolution gratings G190H (1590–2310 Å) and G270H (2220–3275 Å) and the $0.''25 \times 2.''0$ entrance aperture. The spectral resolution with both gratings is roughly 230 km s^{-1} across four pixels. (Note that, although these observations occurred before installation of the image corrector COSTAR, the small aperture prevents significant loss of spectral resolution.) Four exposures with G190H and one with G270H provided total exposure times of 9160 and 1992 seconds, respectively. The individual spectra were calibrated and archived by the Space Telecope Science Institute. I shifted the wavelength scales slightly (<2.0 Å) using the Galactic Mg II absorption lines in the G270H spectra and sharp features common to both the G270H and G190H

Figure 1 shows the combined HST spectrum derived by averaging the individual exposures¹.

3. BAL Profiles

The dotted curve in Figure 1 is a low-order polynomial fit to the continuum, approximately a $\lambda^{-1.5}$ power law. The fit is constrained by the measured flux in 4 narrow wavelength bands, 1980-2030, 2145-2170, 2920-2970 and 3190-3280 Å. The fitted continuum is forced to lie slightly below the observed 3190-3280 Å flux because weak broad emission lines (BELs) of He II λ 1640 and O III] λ 1664 probably contribute at those wavelengths. The fit ignores the numerous intervening (narrow) absorption lines in the 1980-2030 Å band, and it is unconstrained and therefore

highly uncertain at wavelengths below 1980 Å (\lesssim 985 Å rest). Spectra of non-BALQSOs appear to change slope between roughly 1000 and 1200 Å and rise less steeply toward shorter wavelengths than the fit in Figure 1 (Zheng *et al.* 1997). Therefore, the extrapolation of this low-order polynomial probably overestimates the true continuum flux at wavelengths below the O VI BEL.

The final fit in Figure 1 also includes an estimate of the O VI emission line, which appears to be partially absorbed by the P V BAL. The synthesized O VI line has the same redshift and profile as the measured C IV BEL, while its strength is constrained loosely by the measured flux above the fitted continuum on the blue side of the O VI emission profile. The resulting "fit" to the O VI BEL is obviously uncertain, but its strength and profile relative to the other BELs are typical of low-redshift non-BALQSOs (Laor et al. 1994, Laor et al. 1995).

Figure 2 compares several of the line profiles to that of C IV, after normalization by the fit just described. The BALs are "detached" from the emission lines, appearing at velocities between roughly -27,000 and -15,000 km s⁻¹ relative to the emission redshift. There is unrelated absorption at more negative velocities in the N V and O VI profiles caused by blends with other lines (see §4 below). The likely overestimate of the continuum flux across the O VI BAL probably also leads to an overestimate of the absorption strength in this profile.

4. BAL Indentifications

Numerous candidate BALs are labeled in Figure 1 at redshifts corresponding to the 3 deepest minima in the C IV $\lambda\lambda1548,1551$ trough (see Fig. 2). Not all of the labeled transitions are detected. Broad absorption is clearly present in C IV, Si IV $\lambda\lambda1394,1403$, N V $\lambda\lambda1239,1243$, P V $\lambda\lambda1118,1128$, O VI $\lambda\lambda1031,1038$ and probably in Ly α , C III $\lambda977$ and S VI $\lambda\lambda933,945$. Notably absent are significant BALs in the singlyionized lines, Al II $\lambda1671$, C II $\lambda1335$ and Si II $\lambda1260$. Ground-based spectra of PG 1254+047 (Steidel & Sargent 1991) show that Mg II $\lambda\lambda2796,2804$ and Al III $\lambda\lambda1855,1863$ are also not significantly present. This source is therefore among the ma-

¹These manipulations and the fits to the data in §3 were performed with the IRAF software, which is provided by the National Optical Astronomy Observatories under contract to the National Science Foundation.

jority of so-called high-ionization (non-Mg II) BALQSOs. The strengths, profiles and velocities of the BALs in PG 1254+047 are not in any way peculiar for this class of absorber (Junkkarinen *et al.* 1987, Turnshek 1988, Weymann *et al.* 1991, Korista *et al.* 1992).

The normality of this BAL system makes the P V detection particularly interesting. The identification with P V is supported by the excellent redshift and profile coincidences with other BALs (Figs. 1 and 2). The only other transition that might compete with P V near this wavelength is a resonance multiplet of Fe III (UV1), whose ground state transition at 1122.5 Å lies between the P V doublet members. In the only previous secure measurement of a P V BAL (PG 0946+301; Junkkarinen et al. 1997), the P V identification is strongly favored over Fe III because narrow line components provide tight constraints on the expected absorption profiles. In the only known non-BAL system with P V absorption (an intrinsic $z_a \approx z_e$ system in Q 0449-135; Barlow et al. 1997a and 1997b), the much narrower lines confirm the P V identification and rule out any contribution from Fe III. The analogy with these sources suggests that P V is also the correct identification for this feature in PG 1254+047.

However, we can test the P V identifications further by examining the theoretical BAL strengths discussed in §5.2 and §6 below. Figures 4 and 6 (see below) show predicted line optical depths for BALRs that have solar abundances and are in photoionization equilibrium with a standard QSO radiation field. The two plots differ in that Figure 4 assumes the absorber is optically thin in the continuum at all UV wavelengths, while Figure 6 includes significant column densities and therefore continuum opacities. The results are plotted for a range of ionization parameters, U (defined as the dimensionless ratio of the density in hydrogen-ionizing photons to the total hydrogen particle density at the illuminated face of the clouds), where larger U values produce higher ionization states (see §5.2 and §6 for details). The plots are designed to show which lines should appear with P V for roughly solar abundance ratios. However, they also show that Fe III $\lambda 1123$ (in the middle panel of both figures) is much weaker than the

numerous low-ionization lines that are not detected in PG 1254+047, such as Al II λ 1671, Al III $\lambda\lambda 1855,1863$, Mg II $\lambda\lambda 2796,2804$ and C II $\lambda 1335$. In fact, there is no range in U where Fe III $\lambda 1123$ is stronger than the Al II, Mg II and C II lines. Significant absorption in Fe III is therefore effectively ruled out by the absence of the low-ionization lines. Above the ionization limits established below, $\log U \gtrsim -1.8$ in Figure 4 and $\log U \gtrsim -0.6$ in Figure 6, Fe III $\lambda 1123$ is at least \sim 2.7 dex weaker than both P V λ 1118,1128 and the undetected low-ionization lines. Therefore, Fe III cannot contribute to the absorption near 1120 Å without extreme enhancements in the iron abundance. We conclude that P V is the only viable identification for this BAL.

5. Standard Analysis

5.1. Line Optical Depths and Ionic Column Densities

Here I estimate the line optical depths, τ , from the residual intensities, I_r , in the normalized BAL troughs (Fig. 2) using the relation $\tau = -\ln I_r$. Optical depths derived in this way for doublets such as C IV include contributions from both transitions at each velocity. The measured Si IV and possibly P V BALs have absorption structure that corresponds roughly to the doublet separations in these lines (Fig. 2). I therefore use the procedure described by Junkkarinen et al. (1983) to remove the doublet structure and simulate the true run of optical depth versus velocity for single transitions. These corrected optical depth profiles are plotted in Figure 3 for C IV, Si IV and P V. They are directly proportional to the amount of absorbing material (the column density) at each velocity.

Table 1 lists the column densities in C IV, Si IV and P V derived by integrating the optical depth profiles in Figure 3 (with oscillator strengths from Verner et al. 1996). The photon counting statistics and uncertain continuum placements lead to 1σ uncertainties in these column densities of order 0.07 dex for C IV and Si IV and ~ 0.17 dex for P V. Table 1 also provides estimates of the column densities in H I and N V derived by scaling the optical depth profiles in Si IV and C IV to match the

H I and N V BALs, respectively. The C IV optical depths are scaled to fit the observed N V absorption at velocities between roughly -15,500 and -25,000 km s⁻¹, where the measured N V profile should not be seriously contaminated by blends. The scaled C IV profile is then integrated to yield a column density for N V. Similarly, the Si IV optical depth profile is scaled to fit the measured absorption in Ly α near $-24,000 \text{ km s}^{-1}$. The resulting estimate of the H I column density is only an upper limit because the scaling ignores possible contributions from overlapping lines such as Si III. The decision to match the optical depths in N V with C IV and in Ly α with Si IV comes from the assumption that BALs with more similar ionizations have more similar profiles. The 1σ uncertainties in the H I and N V column densities should be ≤ 0.2 dex. Note that the upper limit on the H I column density is consistent with the absence of a strong edge at the Lyman limit (Fig. 1), where optical depth unity would require $\log N_{\rm HI} ({\rm cm}^{-2}) \approx 17.2$.

5.2. Ionization and Total Column Density

The column densities in Table 1 imply that the BALR is optically thin in the Lyman continuum out to at least the N V ionization threshold of 98 eV (see Osterbrock 1989 for bound-free absorption cross-sections). It is therefore appropriate to compare these column densities to theoretical simulations of an optically thin absorbing medium. I use the numerical code CLOUDY (Ferland 1996) to model absorbing regions that 1) are dust-free, 2) have a constant gas density of $n_{\rm H}=10^8~{\rm cm}^{-3},~3)$ have solar element abundances, 4) are optically thin throughout the Lyman continuum, and 5) are in photoionization equilibrium with a standard QSO spectrum. The ionizing spectrum is a piecewise power law $(f_{\nu} \propto \nu^{\alpha})$ with $\alpha = -0.5$ for $0.125 \leq h\nu <$ 25 eV, $\alpha = -2.1$ for $25 \le h\nu < 700$ eV, and $\alpha = -1.0$ for $h\nu \ge 700$ eV. The two-point spectral index between 2500 Å and 2 keV is $\alpha_{ox} =$ -1.5. This continuum shape is C(1.4,-1.5) in the notation of Hamann (1997); it is believed to be appropriate for bright, low-redshift QSOs like PG 1254+047² (but see Zheng et al. 1997 and Korista, Ferland & Baldwin 1997 for discussion). None of the important conclusions would be altered by reasonable changes to the ionizing spectrum (see Hamann 1997). Also, the calculated results of interest here, namely, the ionization fractions at each U, are not sensitive to the density or metal abundances. Therefore, one can use these calculations to derive the abundances in non-solar abundance situations.

Figure 4 shows the calculated line optical depths relative to P V $\lambda 1118$ for all important resonance lines between 912 and 3000 Å (plus Ne VIII $\lambda\lambda770,780$ but excepting lines in the higher H I Lyman series). The oscillator strengths for these calculations are from Verner, Barthel & Tytler (1994). The optical depths are derived assuming that the bound electrons are entirely in their ground states. This is a good approximation for most ions where the first excited levels are at least several eV above ground. However, a few ions have low-energy excited states that could be significantly populated. In those cases, for example C II, Si II, P III and Fe III, the ground and excited state transitions within a given multiplet have similar wavelengths and will be blended in BAL troughs. Therefore, the single-line results in Figure 4 remain good approximations to the total optical depths in the blended multiplets. (For example, the total optical depth in C II $\lambda 1335 +$ C II* $\lambda 1336$ is well approximated by C II $\lambda 1335$ in the figure.)

The most robust, abundance-independent constraints on the ionization come from comparing the measured BALs in different ions of the same element. For PG 1254+047, we can compare C IV with C III and N V with N III. These comparisons are hampered by the line blending and uncertain continuum location at short wavelengths ($\S 3$). Nonetheless, it is clear from Figure 1 that the C IV absorption is stronger (has a larger optical depth) than C III $\lambda 977$ and the

 $^{^2}$ I do not adopt the measured limit of $\alpha_{ox} \leq -1.7$ for PG 1254+047 itself (Wilkes *et al.* 1994) because I will attribute the weak X-ray flux to absorption (§7), consistent with other BALQSOs (§1). The X-ray flux is of little consequence in these calculations anyway, because it has almost no effect on the relative abundances of low-to moderate-ionization species.

N V line is at least several times stronger than N III $\lambda 990$ (which might be absent altogether). Figure 4 shows that this situation requires a minimum ionization parameter of $\log U \gtrsim -1.8$. If the C III BAL is correctly identified, its minimum strength relative to C IV places an upper limit on the ionization. I estimate that the optical depth in C III is at least ~ 0.2 times that in C IV, which implies $\log U \lesssim -1.2$.

These ionization results are consistent with the relative strengths of the BALs of different elements. For example, inspection of Figures 1 and 2 indicates that the optical depths in the N V and O VI troughs are roughly 2 to 5 times larger than those in Si IV. According to Figure 4, this situation requires $-1.7 \lesssim \log U \lesssim -1.5$ for solar abundance ratios among these elements. Similarly, I estimate that the missing low-ionization BALs, Mg II and Al III (Steidel & Sargent 1991), have maximum optical depths of <0.1 if their absorption profiles are similar to Si IV or C IV. The weakness of the low-ionization lines relative to N V and O VI therefore implies $\log U \gtrsim -2.0$.

The simulations used to create Figure 4 also show that the ionization limits inferred from C III/C IV, namely $-1.8 \lesssim \log U \lesssim -1.2$, correspond to neutral hydrogen fractions, $f({\rm H~I}) \equiv N_{\rm HI}/N_{\rm H}$, in the range $-4.0 \lesssim \log f({\rm HI}) \lesssim -3.4$ (see also Figure 2b in Hamann 1997). The upper limit on the H I column density in Table 1 therefore implies a maximum column density in total hydrogen of $18.4 \lesssim \log N_{\rm H}({\rm cm}^{-2}) \lesssim 19.0$, independent of the metal abundances.

5.3. Heavy Element Abundances

The relative abundance of any two elements a and b can be derived from the following equation.

$$\left[\frac{a}{b}\right] = \log\left(\frac{N(a_i)}{N(b_j)}\right) + \log\left(\frac{f(b_j)}{f(a_i)}\right) + \log\left(\frac{b}{a}\right)_{\odot}$$

$$\equiv \log\left(\frac{N(a_i)}{N(b_j)}\right) + IC \tag{1}$$

where $(b/a)_{\odot}$ is the solar abundance ratio, and N and f are respectively the column densities and ionization fractions of elements a and b in

ion stages i and j. IC is the normalized ionization correction factor. Hamann (1997) presented values of IC for a wide range of photoionization conditions in absorbing regions near QSOs. I showed that for optically thin absorbers there are minimum values of IC that can be used to derive minimum metal-to-hydrogen abundance ratios even if there are no constraints on the ionization (see Figures 7-9 in that paper). I also showed that one can make conservatively low (but not quite minimum) estimates of the metal-to-hydrogen ratios by assuming that each metal line forms where that ion is most favored, ie. at U values where the $f(a_i)$ curves are at their peaks (Figure 2b in Hamann 1997). This assumption is most appropriate if there is a range of ionization states caused by a range of densities or distances from the continuum source.

The last two columns in Table 1 give the logarithmic metal-to-hydrogen abundance ratios derived from the measured column densities via Eqn. 1. All of these ratios are lower limits because they are based on an upper limit to the H I column. The results listed for $[M/H]_{min}$ are the absolute minima for each metal M that follow from the minimum IC values (from Figure 9 in Hamann 1997). The results labeled [M/H]_n are the conservatively low ratios derived with the assumption that the $f(M_i)$ curves are at their peaks (with IC from Figure 6 in Hamann 1997). The uncertain shape of the ionizing spectrum causes approximate 1σ uncertainties in the abundances of ± 0.15 dex (not including the uncertainties in the column densities themselves; see Hamann 1997 for discussion).

The same techniques can be used to derive conservatively low, and in some cases minimum, metal-to-metal abundance ratios. Figure 5 shows the values of IC needed to derive [P/C], [P/Si] or [Si/C] abundances from Eqn. 1 given the measured ratios of P V/C IV, P V/Si IV, P IV/Si IV or Si IV/C IV column densities. The correction factors in this plot come from the same photoionization calculations used for Figure 4 (§5.2). We can place a robust lower limit on [P/C] because the P V/C IV correction factor has a firm minimum value of ~ 3.1 (for any ionization state and any nominal continuum shape; see also Fig. 10 in Hamann 1997).

This limit is $[P/C] \gtrsim 2.2$ for the column densities in Table 1. In contrast, the ionization corrections for P V/Si IV and Si IV/C IV depend sharply on U. Above the ionization limit noted above, $\log U \gtrsim -1.8$, I estimate $[P/Si] \lesssim 1.8$ and $[Si/C] \gtrsim 0.5$.

6. Line Saturation: Revised Estimates of the Physical Parameters

The extreme abundances derived in the previous section might be a signal that something is wrong with that analysis. It is already evident from Figure 4 that the variety of BALs observed in PG 1254+047 would be consistent with solar abundances if at least some of the lines are more optically thick than they appear in the spectrum. The line strengths relative to P V provide a test of the saturation hypothesis. In particular, for ionizations above $\log U \geq -1.6$ in Figure 4 there are no BALs clearly absent from PG 1254+047 that have predicted optical depths larger than the P V lines. Conversely, all of the lines with predicted optical depths larger than P V are (or could be) significantly present in the PG 1254+047 spectrum.

If the BALs are saturated, the optical depths and column densities derived in §5.1 and §5.2 are only lower limits and the abundance estimates in §5.3 should be disregarded. The abundance results are corrupted not only by the uncertain column densities, but also by the use of photoionization calculations that assume the absorbing region is optically thin in the UV continuum. That assumption might be incorrect. The larger column densities implied by optically thick lines can produce significant continuous (bound-free) absorption in the BALR which, in turn, leads to a range of ionization states at each U (recall that U applies only to the illuminated face of the clouds). Experiments with CLOUDY show that the results in Figure 4 are accurate for total column densities up to $\log N_{\rm H}({\rm cm}^{-2}) \approx 20.5$; above that, one must examine simulations for particular choices of $N_{\rm H}$.

Figure 6 shows the line optical depths calculated for constant density, photoionized clouds with $N_{\rm H}$ (labeled across the top of the figure) determined at each U by the requirement that the P V BAL ($\lambda 1118+\lambda 1128$) has optical depth

0.2. This P V optical depth is an approximate average over the $\tau_{\rm PV}$ profile in Figure 3 and corresponds to the minimum column density of $\log N_{\rm PV}({\rm cm}^{-2}) \sim 15.0$ in Table 1. The results plotted in Figure 6 are true optical depths (not ratios) for solar abundances and square absorption profiles with FWHM = 10,000 km s⁻¹. Note that total column densities of at least $\log N_{\rm H}({\rm cm}^{-2}) \gtrsim 22.0-[{\rm P/H}]$ are required to reach $\tau_{\rm PV}=0.2$. Also, simulations with $\log U < -1.0$ are not plotted because they have P V optical depths well below 0.2 for any $N_{\rm H}$.

Figure 6 supports the claim that the observed assortment of BALs is consistent with solar abundances if at least some of the lines are optically thick. The observed C III/C IV absorption strengths (§5.2) now require a minimum ionization parameter of $\log U \gtrsim -0.9$, which is also the minimum needed to produce $\tau_{PV} \geq 0.2$. The upper limit on the Mg II absorption, $\tau_{\rm MgII} < 0.1$ (§5.2), relative to P V implies $\log U \gtrsim -0.6$ for roughly solar abundance ratios. If the ionization is high enough, the Si IV line might be optically thin with a column density close to the lower limit in Table 1. However, other minimum optical depths implied by Figure 6 are $\gtrsim 6$ in Ly α , $\gtrsim 25$ in C IV, $\gtrsim 12$ in N V and $\gtrsim 80$ in O VI, which correspond to minimum ionic column densities of $\log N_{\rm HI} ({\rm cm}^{-2}) \gtrsim 16.7 - [{\rm P/H}],$ $\log N_{\rm CIV}({\rm cm}^{-2}) \gtrsim 17.3 - [{\rm P/C}], \log N_{\rm NV}({\rm cm}^{-2}) \gtrsim$ 17.2-[P/N], and $\log N_{\rm OVI}({\rm cm}^{-2}) \gtrsim 18.1-[P/O]$. The scaling of these column densities with the abundance ratios is only approximate because each ion affects the radiative transfer and ionization balance in a different way. Nonetheless, if the abundance ratios are close to solar, the column densities in these ions must be at least an order of magnitude larger than the estimates in Table 1.

If the P V optical depth is larger than the minimum value of 0.2, the $N_{\rm H}$ values in Figure 6 are only lower limits. Adding to the total column densities in those simulations would increase the optical depths in low-ionization lines, such as Mg II and Al III, but leave the high-ionization lines like N V and O VI unchanged. Since Mg II and Al III are the strongest of the low-ionization lines, the upper limits on their optical depths in PG 1254+047 define an upper limit on the total column density at each

U. My estimate of τ < 0.1 for both Mg II and Al III (§5.2) corresponds to maximum column densities of $\log N_{\rm MgII}({\rm cm}^{-2}) < 14.2$ and $\log N_{\rm AlIII}({\rm cm}^{-2}) < 14.4$ for square absorption profiles with FWHM = $10,000 \text{ km s}^{-1}$. Figure 7 compares the envelope of $N_{\rm H}$ upper limits defined by the maximum Mg II and Al III optical depths to the lower limits defined by $\tau_{PV} \geq 0.2$ (from Fig. 6). The range of permitted $N_{\rm H}$ values lies between the two solid curves in Figure 7. The corresponding limits on $N_{\rm HI}$ are shown by the two dash-dot curves in Figure 7. Keeping in mind that $\log N_{\rm HI}({\rm cm}^{-2}) \approx 17.2$ corresponds to optical depth unity at the Lyman limit (Osterbrock 1989), the dash-dot curves indicate that this high-ionization absorber is in all cases optically thin at the Lyman edge (see also Voit et al. 1993).

Obviously, these estimates of the hydrogen column densities depend on the assumption of solar metallicities and, in particular, on solar P/H, Mg/H and Al/H ratios. Higher metal abundances would shift all of the curves in Figure 7 downward. Also, if the line optical depths are greater than expected from the depths of the BALs, then the upper limit on the Mg II and Al III optical depths could be larger than 0.1 and the upper limits on $N_{\rm H}$ and $N_{\rm HI}$ could be larger than they appear in Figure 7. The only firm upper limit on $N_{\rm H}$ comes from the requirement that the absorber is not too optically thick to electron scattering, $\log N_{\rm H}({\rm cm}^{-2}) \lesssim 24.2$ (but see Goodrich 1997).

7. Discussion

The most surprising results from the standard analysis (§5) are the extreme abundance ratios, $[C/H] \gtrsim +1.0$, $[Si/H] \gtrsim +1.8$ and $[P/C] \gtrsim +2.2$. However, I have shown (§6) that the observed BALs are consistent with *solar* metal abundances if at least some of the lines are more optically thick than they appear. This interpretation is supported by the growing evidence for severe saturation in both the broad- and narrow-line intrinsic systems of other QSOs (§1). The large line optical depths are masked in these systems by incomplete line-of-sight coverage of the background emission source(s). Resolved multiplets in narrow-line absorbers can provide both

the coverage fractions and line optical depths (Hamann *et al.* 1997a, Barlow & Sargent 1997). It is therefore significant that the only known narrow-line system with P V absorption also has (resolved) doublet ratios in C IV, Si IV and N V that require line saturation and partial line-ofsight coverage (the P V ratio could not be determined; Barlow et al. 1997a and 1997b). In BALs like PG 1254+047, multiplet ratios are not available and the optical depths and column densities inferred from the absorption troughs must be treated as lower limits. I propose that the significant presence of P V $\lambda\lambda$ 1118,1128 absorption indicates that the optical depths and column densities are much larger than these limits.

One result of the narrow-line studies is that different lines/ions can have different coverage fractions (Hamann et al. 1997a, Barlow et al. 1997a, Barlow & Sargent 1997). No clear picture of the absorbing environments has yet emerged, but the coverage fractions at each profile velocity might depend not only on the geometry but also on the ionization and line optical depths. For example, low-ionization lines might generally have smaller coverage fractions because they form in relatively small and dense condensations within the BALR. Also, even if the BALR has just one ionization state (no dense condensations), different column densities along different sightlines could lead to larger effective coverage fractions in lines that are more optically thick. (Lines of sight through high-column density regions could be optically thick in many transitions – giving rise to the P V absorption and the overall saturated appearance of the spectrum, while sightlines through low-column density gas could be optically thick in just the strongest transitions – giving them larger effective covering.) Some BALs might be weak simply because they are optically thin. However, coverage fractions effects can also produce differences in the BAL strengths and profiles, even among lines that are optically thick. These effects might naturally explain why low ionization BALs like Lyα and Si IV are often weaker (shallower) than, for example, C IV and O VI.

The large line optical depths and possibly complex covering effects imply that we cannot derive elemental abundances from the BALs without a specific physical model. One constraint on such a model is that the partial line-of-sight coverage in PG 1254+047 applies specifically to the continuum source, because some of the strongest and most optically thick BALs (e.g. C IV) are far removed from any emission line. Therefore, either 1) there are physical structures in the BALR smaller than the projected size of the continuum source, which is conservatively <0.01 pc in the standard black hole-accretion disk paradigm (Netzer 1992), or 2) some of the observed continuum flux is scattered into our line of sight without passing through the BALR (Cohen et al. 1995, Goodrich & Miller 1995, Hines & Wills 1995).

Another important result for BALR models is that the high column densities inferred from the P V line will produce significant absorption in soft X-rays (see, for example, the spectral simulations by Shields 1995 and Murray et al. 1995). In fact, the minimum total column density derived here for the BALR, $\log N_{\rm H} ({\rm cm}^{-2}) \gtrsim 22.0$ (Fig. 7), is nearly identical to the minimum absorbing columns inferred from the weak Xray fluxes of other BALQSOs (Green & Mathur 1996). X-ray observations of PG 1254+047 itself (Wilkes et al. 1994) provide upper limits showing that this is also a weak X-ray source consistent with significant X-ray absorption. Its two-point spectral index between 2500 Å and 2 keV is $\alpha_{ox} \leq -1.7 \ (f_{\nu} \propto \nu^{\alpha_{ox}})$, compared to $\alpha_{ox} \leq -1.8$ for BALQSOs in general (Green & Mathur 1996). My calculations (Fig. 7) show that the column densities derived from the only two X-ray detections in BALQSOs, $\log N_{\rm H}({\rm cm}^{-2}) \sim 23$ (Mathur et al. 1995, Green & Mathur 1996), could produce the observed BALs in PG 1254+047 if $+0.4 \le \log U \le +0.7$ in a constant density medium. Therefore, the outflowing BALR is a strong candidate for the X-ray absorber. Furthermore, the profile similarities between P V and strong lines such as C IV, N V and O VI imply that the high column densities (and line saturation) occur across the entire range of absorption velocities, from $-15,000 \text{ to } -27,000 \text{ km s}^{-1}$.

This result for high column densities at high velocities sets stringent requirements for the BALR acceleration. The equation of motion for a wind radiatively driven from a central point source with luminosity L and mass M is,

$$\frac{v\ dv}{dR} = \frac{f_L L}{4\pi R^2 c m_p N_H} - \frac{GM}{R^2} \tag{2}$$

where v is the velocity, R is the radial distance, and f_L is the fraction of the total luminosity absorbed or scattered in the wind. Integrating Equation 2 from R to infinity yields the terminal velocity,

$$v_{\infty} \approx 32000 R_{0.1}^{-\frac{1}{2}} \left(\frac{f_L L_{46}}{N_{22}} - 0.008 M_8 \right)^{\frac{1}{2}} \text{ km s}^{-1}$$
(3)

where $R_{0.1}$ is the inner wind radius in units of 0.1 pc, L_{46} is the QSO luminosity in units of 10^{46} ergs s⁻¹, N_{22} is the total column density in 10^{22} cm⁻², and M_8 is the central black hole mass relative to $10^8~{\rm M}_{\odot}$ (see Scoville & Norman 1995 for similar expressions). $L_{46} \sim 1$ is the Eddington luminosity for $M_8 = 1$, and $R_{0.1} \sim 1$ is a nominal BEL region radius for $L_{46} = 1$ (cf. Peterson 1993). Equations 2 and 3 hold strictly for open geometries, where the photons escaping one location in the BALR are not scattered or absorbed in another location. The radiative force from scattering in a single line is proportional to $1 - e^{-\tau}$; therefore, optically thick lines cannot contribute more to the acceleration as the column densities (and optical depths) increase. However, at high column densities many more lines contribute. My line optical depth calculations for the case where $\tau_{\rm PV} = 0.2 ~(\S6)$ indicate that the enemble BALs scatter $\sim 25\%$ of the continuum flux between 228 and 1600 Å, near the peak of the QSO spectral energy distribution. Considering that there is also bound-free absorption due to helium and the metals, in addition to BALs at shorter wavelengths, it appears that f_L could be as large as a few tenths. Therefore, according to Eqn. 3, the large total column densities implied by the P V analysis (Fig. 7) can be radiatively driven to the observed high velocities. Radiative acceleration becomes even easier if the overall metallicity is above solar, because in that case the derived values of $N_{\rm H}$ would be lower. On the other hand, radiative driving could be problematic if the total column density is as high as $\log N_{\rm H} ({\rm cm}^{-2}) \sim 23.$

Another constraint emerges if we recast Eqn. 3 as a relationship between the velocity and the

ionization parameter, namely,

$$v_{\infty} \lesssim 50 \left(\frac{f_L U \overline{E_{Ryd}}}{V_{fill}} \right)^{\frac{1}{2}} \text{ km s}^{-1}$$
 (4)

where V_{fill} is the volume filling factor (0 \leq $V_{fill} \leq 1$) and $\overline{E_{Ryd}}$ is the average luminosityweighted photon energy in the Lyman continuum in units of Rydbergs. This relationship states simply that the momentum flux in the wind cannot exceed the momentum flux in photons (see also Murray et al. 1995). In conventional small-cloud models of the BALR (Weymann et al. 1985, DeKool 1997), Eqn. 4 shows that radiative acceleration to typical BALR velocities ($\gtrsim 10,000 \text{ km s}^{-1}$) can occur with ionization parameters of $U \lesssim 1$ if $\log V_{fill} \lesssim -4.6$. However, in the recent disk-wind model of Murray et al. (1995) and Murray & Chiang (1996), V_{fill} is unity and extremely high ionization parameters are required to drive the flow. In those models, an additional high-column density absorber is needed to shield the BALR from hard ionizing photons – allowing moderate ionization species to exist at extremely high U in the high-velocity BALR (see Murray et al. 1995). While it appears possible to radiatively drive a $V_{fill} \approx 1$ disk-wind with column densities as large as we infer from the P V absorption (Fig. 7), that scenario requires another X-ray absorber (at low velocities) between the BALR and the continuum source. Murray et al. (1995) showed that the additional absorber must have $\log N_{\rm H}({\rm cm}^{-2}) > 23$ and an ionization high enough to keep the gas optically thin at the Lyman limit.

One final point. I noted in §4 that the BALs in PG 1254+047 are similar to existing measurements of other BALRs. We might, therefore, expect that P V absorption and large column densities are typical of BALQSOs. More and better short-wavelength spectra are needed to search for P V and test the saturation/high column density hypothesis in other sources. The theoretical line optical depths in Figure 6 provide a basis for these tests. Comparing the P V lines to S V, S VI, Ar V or Ar VI transitions might be particularly useful because 1) these species have similar ionizations and 2) enrichment schemes that enhance the odd-numbered elements like phosphorus (Shields 1996) should produce large

P/S and P/Ar abundance ratios (because S and Ar are even). For example, if the P V detections are due to enhanced P abundances then Ar VI $\lambda589$ and $\lambda755$ should be absent, with optical depths $\lesssim 0.01$ times the combined P V doublet for $\log U \lesssim -1.0$ in the calculations of §5.2. In contrast, the saturation/high column density hypothesis favored here predicts (Figure 6b) that these Ar VI lines should be $\gtrsim 0.3$ times the P V pair. Unfortunately, these tests might be thwarted by line blending in most BALQSOs.

8. Summary

I have used HST and ground-based spectra to study the P V $\lambda\lambda1118,1128$ and other broad absorption lines (BALs) in the low-redshift QSO PG 1254+047. The P V identification is secured by this line's redshift and profile similarity to other well-measured BALs, such as C IV $\lambda\lambda1548,1550$ and Si IV $\lambda\lambda1393,1403$, and by photoionization calculations showing that other lines near this wavelength (e.g. Fe III $\lambda1123$) should be much weaker than P V.

A standard analysis (§5), which assumes that the line optical depths and ionic column densities can be derived from the residual intensities in the absorption troughs, leads to the following conclusions; 1) the ionization parameter in the photoionized BALR is $-1.8 \, \lesssim \, \log U \, \lesssim$ -1.2, 2) the total absorbing column is $18.4 \leq$ $\log N_{\rm H}({\rm cm}^{-2}) \lesssim 19.0$, 3) the BALR is optically thin to UV and far-UV continuum radiation, 4) the BALs have optical depths ranging from a few tenths to a few, 6) the BALR has an extremely high metallicity, with $[C/H] \geq$ +1.0 and $[Si/H] \gtrsim +1.8$, and 7) phosphorus is extremely overabundant, with $[P/C] \ge +2.2$. These findings are typical of BALQSOs (§1). The abundance results are particularly interesting because they are incompatible with a well-mixed interstellar medium enriched by a "normal" galactic stellar population (§1 and Hamann 1997); more exotic enrichment schemes are needed (e.g. Shields 1996).

However, the main result of this paper is that the BAL data are consistent with *solar* abundance ratios if at least some of the lines are more optically thick than they appear (§6). In explicit photoionization calculations, the strength of the P V BAL requires minimum line optical depths of $\gtrsim 25$ in C IV, $\gtrsim 12$ in N V and $\gtrsim 80$ in O VI for solar abundance ratios. These minima apply for almost the entire range of BAL velocities, from -15,000 to -27,000 km s⁻¹. The minimum ionization parameter and total column density are $\log U \gtrsim -0.6$ and $\log N_{\rm H} ({\rm cm}^{-2}) \gtrsim 22.0$. In spite of the large column densities, the absence of lowionization lines implies that the absorber is optically thin at the Lyman edge.

I propose that the significant presence of P V absorption is not an indicator of exotic abundances, but rather a byproduct of severe saturation in the other BALs. The large line optical depths are "hidden" in the observed (modest) BAL troughs because the absorber does not fully cover the background continuum source(s) along our line(s) of sight. Differences in the BAL strengths and profiles result from a complex mixture of optical depth, ionization and coverage fraction differences. This interpretation of the BALs in PG 1254+047 is supported by a variety of observational and theoretical studies of intrinsic absorption lines in other QSOs (§1 and §7).

The large column densities inferred from the P V BAL will produce significant bound-free absorption in soft X-rays. The outflowing BALR is therefore a strong candidate for the X-ray absorber in BALQSOs (Mathur et al. 1995, Green & Mathur 1996). In particular, a nominal X-ray absorbing column of $\log N_{\rm H}({\rm cm}^{-2}) \sim 23$ could produce the BAL spectrum in PG 1254+046 if $+0.4 \lesssim \log U \lesssim +0.7$ in a single-zone medium. The predicted line optical depths in Figure 6 provide a basis for testing the high column density hypothesis with future UV spectral observations.

I am grateful to T. A. Barlow and V. T. Junkkarinen for enlightening discussions, and to N. Murray, G. Shields, J. C. Shields and the referee R. Weymann for comments on this manuscript. I also thank G. J. Ferland for his generous support of the CLOUDY software. This work was funded by NASA grants NAG 5-1630 and NAG 5-3234.

 $\begin{tabular}{ll} Table 1 \\ Column Densities and Metal Abundances^a \end{tabular}$

	Ion	$\log N$	$[\mathrm{M/H}]_p$	$[\mathrm{M/H}]_{min}$
•	H I C IV Si IV N V P V	$\lesssim 15.0$ 15.9 15.0 16.2 15.0	+1.4 +2.0 +1.4 +3.3	+1.0 +1.8 +1.0 +3.1

^aMetal abundances are $[M/H]_p$ for $f(M_i)$ at their peaks and $[M/H]_{min}$ for the minimum IC. Column densities are in cm⁻². See §5.1 and §5.3.

REFERENCES

- Arav, N. 1997, in Mass Ejection From AGN, eds. R. Weymann, I. Shlosman, and N. Arav, ASP Conf. Series, 128, 208
- Bahcall, J. N., et al. 1993, ApJS, 87, 1
- Barlow, T. A., et al. 1997b, in prep.
- Barlow, T. A., Hamann, F., & Sargent, W. L.
 W. 1997a, in Mass Ejection From AGN, eds.
 R. Weymann, I. Shlosman, and N. Arav, ASP
 Conf. Series, 128, 13
- Barlow, T. A., & Junkkarinen, V. T. 1994, BAAS, 26, 1339
- Barlow, T. A., & Sargent, W. L. W. 1997, AJ, 113, 136
- Cohen, M. H., Ogle, P. M., Tran, H. D., Vermeulen, R. C., Miller, J. S., Goodrich, R. W., & Martel, A. R. 1995, ApJ, 448, L77
- DeKool, M. 1997, in Mass Ejection From AGN, eds. R. Weymann, I. Shlosman, and N. Arav, ASP Conf. Series, 128, 233
- Ferland, G. J. 1996 HAZY, a Brief Introduction to Cloudy, University of Kentucky, Department of Physics and Astronomy, Internal Report
- Foltz, C. B., Chaffee, F. H., Hewett, P. C., Weymann, R. J., & Morris, S. L. 1990, BAAS, 2, 806
- George, I. M., Turner, T. J., Netzer, H., Nandra, K., Mushotzky, R. F., & Yaqoob, T. 1997, ApJS, in press
- Goodrich, R. W. 1997, ApJ, 474, 606
- Goodrich, R. W., & Miller, J. S. 1995, ApJ, 448, L73
- Green, P. J., Aldcroft, T. L., Mathur, S., & Shartel, N. 1997, ApJ, in press
- Green, P. J., & Mathur, S. 1996, ApJ, 462, 637
- Hamann, F. 1997, ApJS, 109, 279
- Hamann, F., Barlow, T. A., Beaver, E. A., Burbidge, E. M., Cohen, R. D., Junkkarinen, V., & Lyons, R. 1995, ApJ, 443, 606

- Hamann, F., Barlow, T. A., Junkkarinen, V. T.,& Burbidge, E. M. 1997a, ApJ, 478, 80
- Hamann, F., Barlow, T. A., & Junkkarinen, V.T. 1997b, ApJ, 478, 87
- Hamann, F., Barlow, T. A., Cohen, R. D.,
 Junkkarinen, V. T., & Burbidge, E. M. 1997c,
 in Mass Ejection From AGN, eds. R. Weymann, I. Shlosman, and N. Arav, ASP Conf.
 Series, 128, 19
- Hamann, F., & Ferland, G. J. 1993, ApJ, 418,
- Hewitt, D. & Burbidge, G. 1993, ApJS, 87, 451
- Hines, D. C., & Wills, B. J. 1995, ApJ, 448, L69
- Junkkarinen, V. T., Beaver, E. A., Burbidge,
 E. M., Cohen, R. D., & Hamann, F. 1997, in
 Mass Ejection From AGN, eds. R. Weymann,
 I. Shlosman, and N. Arav, ASP Conf. Series,
 128, 220
- Junkkarinen, V. T., Beaver, E. A., Burbidge, E. M., Cohen, R. D., Hamann, F., Lyons, R. W., & Barlow T. A. 1995, BAAS, 27, 872
- Junkkarinen, V. T., Burbidge, E. M., & Smith, H. E. 1983, ApJ, 265, 51
- Junkkarinen, V. T., Burbidge, E. M., & Smith, H. E. 1987, ApJ, 317, 460
- Kopko, M. Jr., Turnshek, D. A., & Espey, B. R. 1994, in IAU Symp. 159, Multi-Wavelength Continuum Emission of AGN, eds. T. J.-L. Courvoisier & A. Blecha (Dordrecht:Kluwar), 450
- Korista, K. T., Ferland, G., & Baldwin, J. 1997, ApJ, in press
- Korista, K. T., Hamann, F., Ferguson, J., & Ferland, G. J. 1996, ApJ, 461, 641
- Korista, K. T., Weymann, R. J., Morris, S. L., Kopko, M., Jr., Turnshek, D. A., Hartig, G. F., Foltz, C. B., Burbidge, E. M., & Junkkarinen, V. T. 1992, ApJ, 401, 529
- Laor, A., Bahcall, J. N., Jannuzi, B. T., Schneider, D. P., Green, R. F., & Hartig, G. F. 1994, ApJ, 420, 110

- Laor, A., Bahcall, J. N., Jannuzi, B. T., Schneider, D. P., Green, R. F., & Hartig, G. F. 1995, ApJS, 99, 1
- Laor, A., Fiore, F., Elvis, M., Wilkes, B. J., & McDowell, J. C. 1997, ApJ, 477, 93
- Mathur, S. 1994, ApJ, 431, L75
- Mathur, S., Wilkes, B., Elvis, M., & Fiore, F. 1994, ApJ, 434, 493
- Mathur, S., Elvis, M., & Singh, K. P. 1995, ApJ, 455, L9
- Murray, N., & Chiang, J. 1995, ApJ, 454, L105
- Murray, N., Chiang, J., Grossman, S. A., & Voit, G. M. 1995, ApJ, 451, 498
- Netzer, H. 1992, in Testing the AGN Paradigm, AIP Conf. Proc. 254, Eds. Stephan S. Holt, Susan G. Neff, & C. Megan Urry, p. 146
- Osterbrock, D. E. 1989, Astrophysics of Gaseous Nebulae and Active Galactic Nuclei, (Mill Valley:University Science Books), p. 36
- Peterson, B. 1993, PASP, 105, 247
- Petitjean, P., Rauch, M., & Carswell, R. F. 1994, A&A, 291, 29
- Reynolds, C. S. 1997, MNRAS, 286, 513
- Scoville, N., & Norman, C. 1995, ApJ, 451, 510
- Shields, G. A., 1996, ApJ, 461, L9
- Shields, J. C. 1995, in Reverberation Mapping of the Broad-Line Region of Active Galactic Nuclei, eds. P. M. Gondhalekar, K. Horne, and B. M. Peterson, (San Francisco: ASP), xx
- Singh, K. P., Westergaard, N. J., & Schnopper, H. W. 1987, A&A, 172, L11
- Steidel, C. C., & Sargent, W. L. W. 1991, ApJ, 382, 433
- Turnshek, D. A. 1984, ApJ, 280, 51
- Turnshek, D. A. 1988, in QSO Absorption Lines:
 Probing the Universe, eds. J. C. Blades, D.
 A. Turnshek, & C. A. Norman (Cambridge: Cambridge Univ. Press), 17

- Turnshek, D. A. 1995, in QSO Absorption Lines, ed. G. Meylan, (Berlin:Springer-Verlag), 223
- Turnshek, D. A., Kopko, M., Monier, E., Noll, D., Espey, B., & Weymann, R. J. 1996, ApJ, 463, 110
- Verner, D., Barthel, P. D., & Tytler, D. 1994, A&AS, 108, 287
- Verner, D., Verner, E. M., & Ferland, G. J. 1996, Atomic Data and Nuclear Data Tables, 64, 1
- Voit, G. M., Weymann, R. J., & Korista, K. T. 1993, ApJ, 413, 95
- Wampler, E. J., Bergeron, J., & Petitjean, P. 1993, A&A, 273, 15
- Wampler, E. J., Chigai, N. N., & Petitjean, P. 1995, ApJ, 443, 586
- Weymann, R. J. 1995, in QSO Absorption Lines, ed. G. Meylan, (Berlin:Springer-Verlag), 213
- Weymann, R. J., Morris, S. L., Foltz, C. B., & Hewett, P. C. 1991, ApJ, 373, 23
- Weymann, R. J., Turnshek, D. A., & Christiansen, W. A. 1985, in Astrophysics of Active Galaxies and Quasi-Stellar Objects, ed. J. Miler, (Mill Valley:Univ. Sci. Books), 185
- Wilkes, B. J., Tananbaum, H., Worrall, D. M., Avni, Y., Oey, M. S., & Flanagan, J. 1994, ApJS, 92, 53
- Zheng, W., Kriss, G. A., Telfer, R. C., Grimes, J. P., & Davidson, A. F. 1997, ApJ, 475, 469

This 2-column preprint was prepared with the AAS IAT_FX macros v4.0.

FIGURE CAPTIONS

Fig. 1. — HST spectrum of PG 1254+047 at the observed wavelengths. The Flux has units 10^{-15} ergs s⁻¹ cm⁻² Å⁻¹. The 1- σ uncertainties are plotted across the bottom. The emission lines are labeled at $z_e=1.010$ across the top. The wavelengths of possible BALs are labeled at 3 redshifts, $z_a=0.855,\,0.871$ and 0.893, corresponding to the 3 deepest minima in the C IV trough. The label LL marks the position of the H I Lyman limit (912 Å). Not all of these labeled features are present. The smooth dotted curve is a fit to the continuum that includes a synthetic O VI emission profile (see §2 and §3).

Fig. 2. — Line profiles are plotted on a velocity scale relative to the emission redshift $z_e = 1.010$. The thin curve in each panel is the C IV profile, while the thick curves are from top to bottom Si IV, N V, P V and O VI. The velocities of these doublets are defined by the equal-weight average of the individual rest wavelengths. The horizontal bar near the top-center of each panel shows the doublet separations. The C IV separation (not shown) is negligible on this scale ($\sim 500 \text{ km s}^{-1}$). Note that the plots often include unrelated emission or absorption lines (§3).

Fig. 3. — BAL optical depth profiles derived from the observed residual intensities using an algorithm that approximately removes the doublet structure (see §5.1).

Fig. 4. — Theoretical line optical depths relative to P V $\lambda 1118$, $\tau/\tau(\lambda 1118)$, are plotted for solar abundances and different values of the ionization parameter, U, in optically thin clouds that are photoionized by a standard QSO continuum. The 3 panels show lines appearing at different wavelengths: $912 \le \lambda < 1025 \text{ Å}$ (left panel), $1025 \le \lambda < 1220 \text{ Å (middle)}$ and $1220 \le \lambda < 3000 \text{ Å (right)}$. The plots include all resonance lines at these wavelengths with the exceptions of the high-level H I lines and numerous low-ionization lines that would fill in the lower left corner of each panel. The 2 thick horizontal curves in all 3 panels are the normalized optical depths in the P V doublet, $\lambda\lambda 1118,1128$. The absolute optical depths in the stronger P V

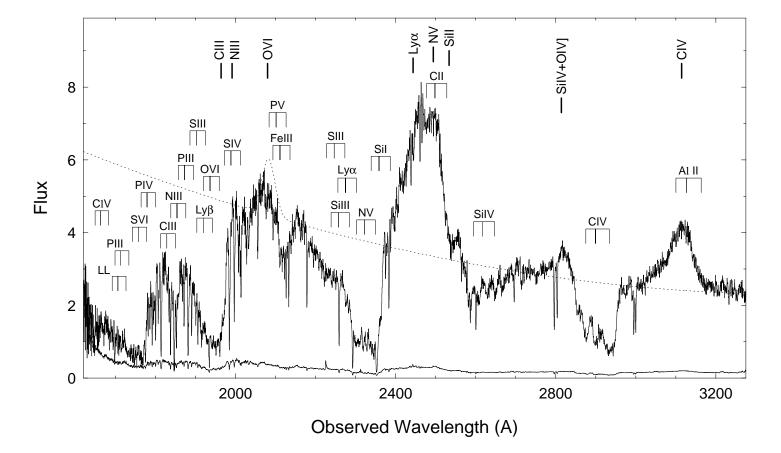
transition, $\lambda 1118$, are labeled across the top for $N_{\rm H} = 10^{20} \ {\rm cm^{-2}}$ and a square absorption profile with FWHM = 10,000 km s⁻¹. See §3 and §5.2.

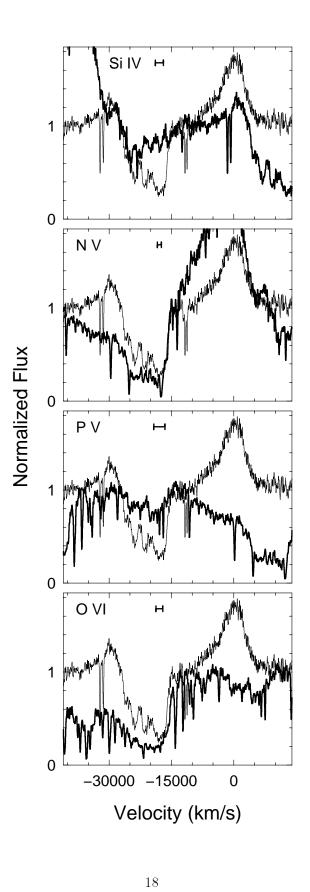
Fig. 5. — Logarithmic ionization corrections normalized to solar abundances, IC, are plotted for various ionization parameters, U, in calculations identical to Figure 4. The curve labeled P V/C IV gives the correction factor for deriving the [P/C] abundance from Equation 1, etc.. The curve for P V/Si IV is shifted up by +1 for convenience.

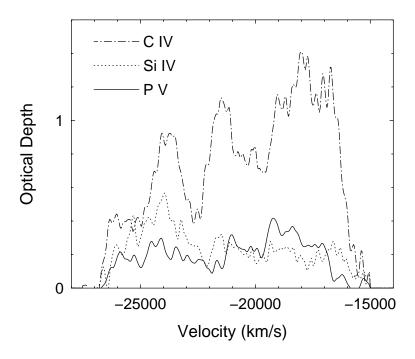
Fig. 6a. — Theoretical line optical depths, τ , for constant density, photoionized clouds that have solar abundances and square absorption profiles with FWHM = 10,000 km s⁻¹. The total column density, $N_{\rm H}$ (labeled across the top), at each ionization parameter, U (bottom), is adjusted so that the optical depth in P V (λ 1118+ λ 1128) equals 0.2. The P V optical depths fall below this mark at $\log U = -1.0$ because no value of $N_{\rm H}$ can achieve $\tau_{\rm PV} = 0.2$ for $\log U \lesssim -1.0$. The 3 panels show all resonance lines of significant strength between 912 and 3000 Å, as in Figure 4 (again excluding numerous low-ionization lines that would fill in the lower left corner of each panel).

Fig. 6b. — Same as Figure 6a except for lines at shorter wavelengths: $584 \le \lambda < 675 \text{ Å}$ (left panel), $675 \le \lambda < 750 \text{ Å}$ (middle) and $750 < \lambda < 912 \text{ Å}$ (right).

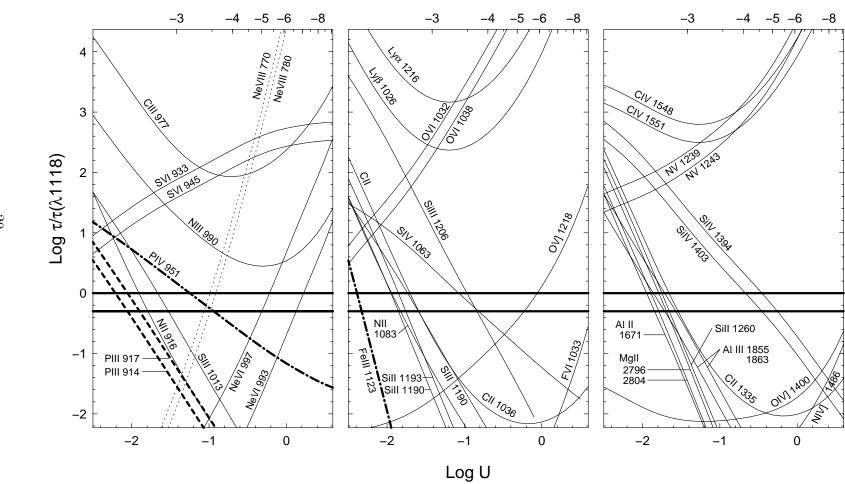
Fig. 7. — Column density limits for $N_{\rm H}$ (solid curves, left-hand scale) and $N_{\rm HI}$ (dashdot curves, right-hand scale) for different ionization parameters, U, in constant density, photoionized clouds with solar abundances. The minimum $N_{\rm H}$ and $N_{\rm HI}$ values (lower curves for $\log U \gtrsim -0.6$) derive from the requirement that $\tau_{PV} \geq 0.2$, while the maximum values (upper curves) follow from $\tau_{\rm MgII}$ and $\tau_{\rm AlIII} \leq 0.1$. The permitted values of $N_{\rm H}$ and $N_{\rm HI}$ lie between the two pairs of curves for $\log U \gtrsim -0.6$, as indicated by the arrows (see §6).











Log $\tau(\lambda 1118)$

